Rotational viscosity of fluids composed of linear molecules: An equilibrium molecular dynamics study

R. J. D. Moore, J. S. Hansen,[a] and B. D. Todd
Centre for Molecular Simulation, Swinburne University of Technology, P.O. Box 218, Hawthorn, Victoria 3122, Australia

(Received 26 February 2008; accepted 17 April 2008; published online 10 June 2008)

In this paper, we investigate the rotational viscosity for a chlorine fluid and for a fluid composed of small linear molecules by using equilibrium molecular dynamics simulations. The rotational viscosity is calculated over a large range of state points. It is found that the rotational viscosity is almost independent of temperature in the range studied here but exhibits a power-law dependency on density. The rotational viscosity also shows a power-law relationship with the molecular length, and the ratio between the shear and rotational viscosities approaches 0.5 for the longest molecule studied here. By changing the number of atoms or united atomic units per molecule and by keeping the molecule length fixed, we show that fluids composed of molecules which have a rodlike shape have a lower rotational viscosity. We argue that this phenomenon is due to the reduction in intermolecular connectivity, which leads to larger fluctuations around the values possessed by the fluid on average. The conclusions here can be extended to fluids composed of uniaxial molecules of arbitrary length. © *2008 American Institute of Physics*. [DOI: 10.1063/1.2921135]

I. INTRODUCTION

Classical fluid dynamics is concerned with the spatiotemporal behavior of fluid translational momentum, energy, and density. Fluid dynamics can successfully describe many phenomena; however, in its classical formulation, it is rather coarse grained in that many microscopic degrees of freedom and their coupling to the macroscopic quantities are ignored. It is well-known that for molecular fluids, the intrinsic angular momentum (or molecular spin) couples to the fluid translational velocity.[1–3] This coupling is ignored in the classical fluid dynamics approach but should, at least in principle, be included into the dynamical description.

For a fluid composed of uniaxial molecules, a thermodynamical force arises if the angular velocity of the fluid $\boldsymbol{\Omega}$ does not resemble that of a rigid body[4] where the following is true,

$$2\boldsymbol{\Omega} = \nabla \times \mathbf{u}, \tag{1}$$

where $\mathbf{u}$ is the velocity field.[1,5] The force, which is sometimes referred to as the sprain rate,[5] will lead to a conjugated flux through the linear constitutive relation[1]

$$\overset{d}{\mathbf{P}} = -\eta_r(\nabla \times \mathbf{u} - 2\boldsymbol{\Omega}), \tag{2}$$

where $\overset{d}{\mathbf{P}}$ is the vector dual of the antisymmetric part of the pressure tensor and η_r is the rotational viscosity. Thus, the rotational viscosity is a transport coefficient that describes the decay of the antisymmetric stress after an infinitely small perturbation away from the condition given in Eq. (1). By applying the constitutive relation [Eq. (2)] to the balance equations, which also include an equation describing the dynamics of the intrinsic angular momentum, it can be shown that the rotational viscosity also accounts for coupling between the angular velocity and the translational motion of the fluid.[1] For steady flows, e.g., a low Reynolds number Poiseuille flow, this coupling can be safely ignored.[6] However, for anisotropic fluids, e.g., nematic fluids[7] and unsteady flows,[6] it can have a very large effect on the overall dynamics of the system.

Since a complete dynamical description of a molecular fluid includes the molecular spin, the rotational viscosity must be evaluated alongside the other transport coefficients. Some experimental methods have been advised,[8] which use rotating magnetic or electrical fields but are rather involved. Evans and Hanley[9] were the first to compute the rotational viscosity of chlorine by using the solution to the generalized Langevin equation and molecular dynamics (MD) simulations. Edberg *et al.*[5] and, more recently, Delhommelle[10] have also studied chlorine via MD and included the dependence of the rotational viscosity on the intrinsic angular velocity. Allen *et al.*[11] have deduced analytical expressions for the rotational viscosity for hard convex bodies. For nematic liquid crystals composed of relatively large molecules with molecular weight in the order of 250 g/mol, Zakharov *et al.*[12] and also Capar and Cebe[13] have studied the rotational viscosity as a function of temperature by using MD. To the best of our knowledge, no one has yet published any systematic study of the rotational viscosity as a function of density and temperature and for different molecular fluids. It is the purpose of this paper to do just that by using equilibrium MD simulations where these parameters can be easily controlled. We will only focus on fluids composed of small linear molecules comprising two to four atoms, or united atomic units (UAUs), where Eq. (2) applies. To keep this study as general

[a]Author to whom correspondence should be addressed. Electronic mail: jhansen@ict.swin.edu.au.

TABLE I. Simulation parameters for Cl_2. l_{mol} is given by the end-to-end distance of the molecules. The corresponding rotational temperature is $T_r = 0.73 \pm 0.05$

	Cl_2 molecules
Number of molecules	256
N_{UAU}	2
l_{mol}	0.63 ± 0.03
L-J cutoff	2.5 (unshifted)
Temperature	0.96 ± 0.03
UAU number density	1.088
Time step	0.001

as possible, we will allow small amplitude bond length and bending angle vibrations and we shall limit ourselves to study only two different molecular fluids, namely, chlorine and a generic fluid where the number of UAUs per molecule can be varied.

The paper is organized as follows. In the next section, we present the molecular model and the details concerning the MD simulations. In this section, we also show in detail how the rotational viscosity is calculated based on the method provided by Evans and Hanley.[9] In Sec. III, the results from the simulations are presented and discussed, and finally, we make a few concluding and perspective remarks.

II. METHODOLOGY

A. Molecular model and simulation details

We have chosen a linear molecular model that includes pair potential interactions, bond stretching interactions between bonded UAU, as well as bending force interactions. The total potential energy in the system can then be written as

$$U = \sum_{\text{pairs}} U_p(r_{ab}) + \sum_{\text{bonds}} U_b(r_{ab}) + \sum_{\text{angles}} U_a(\theta). \tag{3}$$

Here, r_{ab} is the absolute distance between UAUs a and b and θ is the angle between two bonds that are connected to the same UAU. The first sum on the right hand side runs over all pairs of UAUs that are not connected via a bond; i.e., two bonded UAU only interact via the stretching potential. The functional form of the potential governing the pair interactions U_p is of the Lennard-Jones type,

$$U_p(r_{ab}) = \begin{cases} 4\epsilon\left[\left(\frac{\sigma}{r_{ab}}\right)^{12} - \left(\frac{\sigma}{r_{ab}}\right)^{6}\right] & \text{if } r_{ab} \leqslant r_c \\ 0 & \text{otherwise,} \end{cases} \tag{4}$$

where, as stated above, UAUs a and b are not bonded and can belong to the same or different molecule. σ is a length scale and ϵ is an energy scale. For chlorine, for example, $\sigma = 3.332 \times 10^{-10}$ m and $\epsilon = 2.462 \times 10^{-21}$ J.[14] We will use two different values for the critical cutoff length r_c. For chlorine, we set $r_c = 2.5\sigma$, and for the generic molecule, we use $r_c = 2^{1/6}\sigma$. In the latter case, the potential function is also shifted upwards such that $U_p(r_c) = 0$, which is the Weeks–Chandler–Andersen (WCA) potential.[15] For us to make a comparison with previous work, we will leave the potential unshifted for chlorine. The bond stretching potential is given by a simple spring potential,

$$U_b(r_{ab}) = \tfrac{1}{2}k_s(r_{ab} - l_{\text{bond}})^2, \tag{5}$$

where k_s is the spring constant and l_{bond} is the mean (or equilibrium) bond length. The bending potential used is that typically applied for alkanes,[16,17]

$$U_a(\theta) = \tfrac{1}{2}k_\theta(\cos(\theta) - \cos(\theta_0)), \tag{6}$$

where θ_0 is the equilibrium bending angle and k_θ is the bending constant.

A comment about the choice of model is in place. For low weight molecules such as N_2 and Cl_2, the bond stretching interactions are typically not explicitly included due to the high frequency vibrations and, therefore, long simulation times. Furthermore, for very low weight molecules, e.g., H_2, the bond vibrations should also be treated as a quantum phenomenon. In such cases, the bond length is kept fixed either by solving Lagrangian equations of motion or by applying a relaxation method.[18] Here, we wish to study the general case where the UAU may have a considerable mass and where the bond vibrations should be included. There is also a computational benefit: we have found that using the SHAKE algorithm[18] to keep the bond fixed, with an error tolerance of $1 \times 10^{-6}\sigma$, increases the simulation time by around 12% compared to including the bond interaction explicitly using a time step that ensures the same standard error in energy conservation. It must, however, be stressed that one does not obtain the same dynamics by simply letting $k_s \to \infty$,[18] and it is, therefore, important to investigate the possible effects of varying k_s. We shall comment on this later.

One can express any physical quantity in units of σ, ϵ, and mass m. Thus, the temperature T can be expressed in dimensionless (or reduced) units as $T^* = k_B T/\epsilon$, number density as $\rho^* = \rho\sigma^3$, time as $t^* = t/(\sigma\sqrt{m/\epsilon})$, and so forth. Here, k_B is the Boltzmann constant. We will, as is common practice, for the remainder of the paper, express all quantities in reduced units and drop the asterisk altogether.

The MD simulations were carried out in the *NVE* ensemble after an equilibration period, where the system was thermostated to a desired temperature. Throughout the simulation, the equations of motion were integrated forward in time by using a leap-frog integration scheme,[19] with a time step of $\Delta t = 0.001$, and periodic boundary conditions were used in all directions. The force calculations were performed by implementing the potential functions using the algorithms given in the works of Allen and Tildesley[20] and Rapaport.[17] The number of UAUs in the simulation box varied from 512 to 1728 depending on the molecular fluid simulated. It was verified that the transport coefficients were not affected by the system size within statistical uncertainty. For systems where the number of UAUs per molecule N_{UAU} was greater than 2, the equilibrium bending angle was set such that $\theta \approx \pi$, which stretches out the molecule and gives close to a uniaxial shape. We will use $k_\theta = 500$ throughout the paper.

Two series of simulations were carried out. In the first, the rotational viscosity of chlorine was calculated for different state points. This enables a comparison of our data with previously published values. The second series of simula-

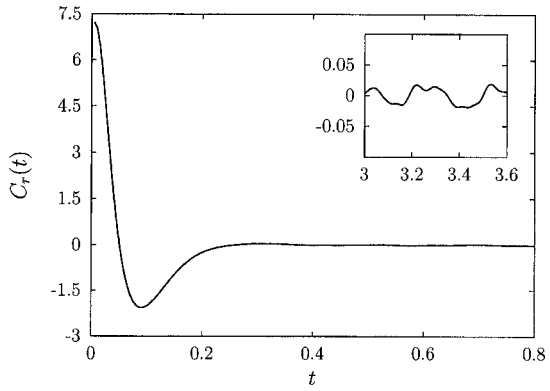

FIG. 1. Autocorrelation function of the antisymmetric part of the pressure tensor for Cl_2 with $k_s=5000$ as a function of time at S1. Note that the autocorrelation function has decayed to approximately zero for $t>0.5$. The inset shows the fluctuations around zero of the autocorrelation function for later times.

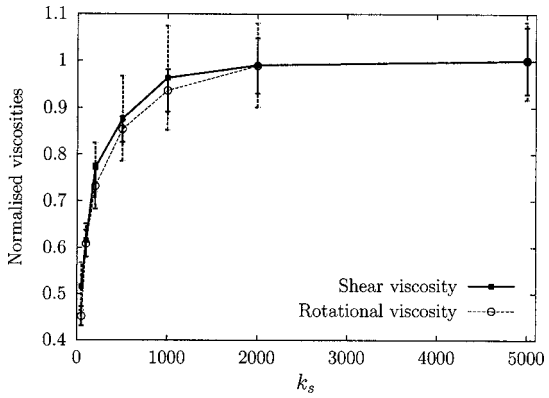

FIG. 3. Normalized shear and rotational viscosities as a function of bond stiffness for Cl_2 at S1. Viscosities are normalized by their maximum values to highlight the similarities between the dependence of shear and rotational viscosities on bond stiffness. The lines serve as a guide for the eyes.

tions focused on the generic molecular fluid where the bond length and N_{UAU} are varied to study the effects these have on the rotational viscosity.

B. Evaluation of the viscosities

The viscosities are evaluated by using the Green–Kubo integral of the autocorrelation functions of the symmetric and antisymmetric parts of the molecular pressure tensor.[21] On a microscopic scale, the pressure tensor is defined as[20]

$$\mathsf{P}=\frac{1}{V}\left[\sum_i \frac{\mathbf{p}_i\mathbf{p}_i}{M_i}+\sum_i\sum_{i<j}\mathbf{r}_{ij}\mathbf{F}_{ij}\right], \tag{7}$$

where V is the system volume, $\mathbf{p}_i$ is the momentum of the center of mass of molecule i, M_i is the mass, and $\mathbf{r}_{ij}=\mathbf{r}_i-\mathbf{r}_j$, where $\mathbf{r}_i$ and $\mathbf{r}_j$ are the centers of mass of molecules i and j, respectively. The force acting between molecules i and j, $\mathbf{F}_{ij}$, is given by

$$\mathbf{F}_{ij}=\sum_{a\in i}\sum_{b\in j}\mathbf{F}_{ab}, \tag{8}$$

where $\mathbf{F}_{ab}$ is the force acting between UAU a in molecule i and UAU b in j. The pressure tensor can be decomposed into a traceless symmetric part $\overset{\mathrm{os}}{\mathsf{P}}$ and an antisymmetric part $\overset{a}{\mathsf{P}}$, i.e.,

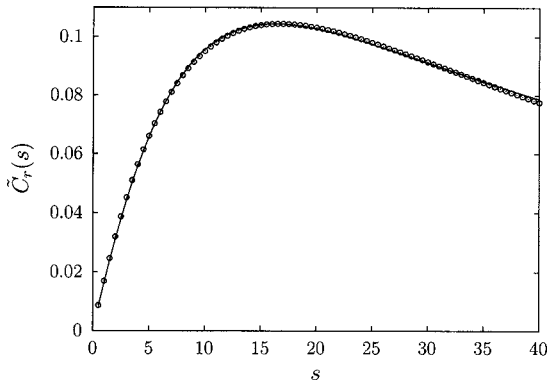

FIG. 2. Fit of Eq. (14) (full line) applied to the Laplace transform of the MD data given in Fig. 1 (circles).

$$\mathsf{P}=p\mathsf{I}+\overset{\mathrm{os}}{\mathsf{P}}+\overset{a}{\mathsf{P}}. \tag{9}$$

Here, p is the pressure given by the average of the trace of P, $p=\mathrm{tr}(\mathsf{P})/3$, $\overset{\mathrm{os}}{\mathsf{P}}=\frac{1}{2}(\mathsf{P}+\mathsf{P}^T)-p$, and $\overset{a}{\mathsf{P}}=\frac{1}{2}(\mathsf{P}-\mathsf{P}^T)$. The zero frequency zero wave vector shear viscosity is then directly evaluated by using the standard Green–Kubo integral,[22]

$$\eta_0=\frac{V}{3k_BT}\int_0^\infty\left\langle\sum_{\alpha\beta}\overset{\mathrm{os}}{P}_{\alpha\beta}(0)\overset{\mathrm{os}}{P}_{\alpha\beta}(t)\right\rangle dt, \tag{10}$$

where we explicitly indicate the time dependence and $\alpha\beta$ runs over the xy, xz, and yz elements of $\overset{\mathrm{os}}{\mathsf{P}}$.

The molecular spin angular momentum is a nonconserved quantity, since only the total angular momentum is conserved. This, in turn, means that the rotational viscosity cannot be directly calculated from a Green–Kubo integral of the autocorrelation function of $\overset{a}{\mathsf{P}}$.[9] However, by solving the generalized Langevin equation, the Laplace transform of the rotational viscosity is given as[9,23]

$$\tilde{\eta}_r(s)=\frac{\tilde{C}_r(s)}{1-\dfrac{1}{\rho\Theta}\dfrac{\tilde{C}_r(s)}{s}}, \tag{11}$$

where Θ is the average of the trace of the moment of inertia tensor per unit mass and $\tilde{C}_r(s)$ is the Laplace transform of the

TABLE II. Simulation results for Cl_2 at S1. Corroboratory results were obtained by using rigid intramolecular bonds, whereas our results were obtained with a bond stiffness $k_s=5000$. The shear viscosity quoted from Matin *et al.* (Ref. 14) has been extrapolated from their reported results. Our uncertainties stated in this report are equal to the 95.4% confidence bounds obtained from ten runs. Each run is averaged over 1000 samples.

	P	η_0	η_r
Matin *et al.*[a]	1.31	$\sim 7.0\pm 0.5$	⋯
Delhommelle[b]	1.29 ± 0.1	⋯	0.47 ± 0.02
This work	1.21 ± 0.56	6.71 ± 0.55	0.42 ± 0.03

[a]Reference 14.
[b]Reference 10.

TABLE III. Summary of the l_{mol}, η_0, and η_r data collected for Cl_2 at $T=1.5, 3.0, 4.5$.

	$T=1.5$			$T=3.0$			$T=4.5$		
ρ	l_{mol}	η_0	η_r	l_{mol}	η_0	η_r	l_{mol}	η_0	η_r
0.44	0.62 ± 0.01	0.30 ± 0.07	0.05 ± 0.00	0.64 ± 0.01	0.48 ± 0.19	0.03 ± 0.01	0.65 ± 0.01	0.60 ± 0.14	0.03 ± 0.00
0.52	0.63 ± 0.01	0.48 ± 0.09	0.06 ± 0.00				0.65 ± 0.01	0.69 ± 0.17	0.04 ± 0.01
0.60	0.63 ± 0.01	0.63 ± 0.10	0.07 ± 0.00	0.64 ± 0.01	0.72 ± 0.14	0.06 ± 0.01	0.65 ± 0.01	0.85 ± 0.09	0.06 ± 0.00
0.68	0.63 ± 0.01	0.82 ± 0.14	0.09 ± 0.00	0.64 ± 0.01[a]	1.04 ± 0.22[a]	0.09 ± 0.01[a]	0.64 ± 0.01	1.07 ± 0.15	0.08 ± 0.01
0.76	0.63 ± 0.01	1.15 ± 0.14	0.11 ± 0.01				0.64 ± 0.01	1.37 ± 0.21	0.11 ± 0.01
0.84	0.63 ± 0.01	1.54 ± 0.23	0.14 ± 0.01	0.63 ± 0.01[b]	1.40 ± 0.29[b]	0.13 ± 0.01[b]	0.63 ± 0.01	1.69 ± 0.22	0.14 ± 0.01
0.92	0.62 ± 0.01	2.11 ± 0.23	0.19 ± 0.00	0.62 ± 0.01[c]	1.91 ± 0.33[c]	0.19 ± 0.02[c]	0.62 ± 0.01	2.27 ± 0.41	0.19 ± 0.02
1.00	0.62 ± 0.01	3.01 ± 0.41	0.25 ± 0.01	0.61 ± 0.01	2.80 ± 0.25	0.26 ± 0.01	0.61 ± 0.01	2.85 ± 0.40	0.24 ± 0.02
1.088	0.61 ± 0.01	4.65 ± 0.27	0.34 ± 0.01	0.60 ± 0.01	3.80 ± 0.42	0.34 ± 0.02	0.60 ± 0.01	3.52 ± 0.70	0.30 ± 0.01
1.16	0.60 ± 0.01	7.10 ± 0.43	0.41 ± 0.01	0.59 ± 0.01	5.14 ± 0.78	0.37 ± 0.02	0.59 ± 0.01	4.74 ± 0.43	0.35 ± 0.02

[a]Data were collected at $\rho=0.70$.
[b]Data were collected at $\rho=0.80$.
[c]Data were collected at $\rho=0.90$.

autocorrelation function of the antisymmetric part of the pressure tensor. We may write $\tilde{C}_r(s)$ as

$$\tilde{C}_r(s)=\frac{V}{3k_BT}\int_0^\infty \langle \overset{d}{\mathbf{P}}(0)\cdot\overset{d}{\mathbf{P}}(t)\rangle e^{-st}dt, \tag{12}$$

where $\overset{d}{\mathbf{P}}$ is the vector dual of $\overset{a}{\mathsf{P}}$, as mentioned in Sec. I, and can be found by $\overset{d}{\mathbf{P}}=\boldsymbol{\epsilon}:\overset{a}{\mathsf{P}}$, where $\boldsymbol{\epsilon}$ is the third order Levi–Civita tensor. Due to the term $\tilde{C}_r(s)/s$ in the denominator of Eq. (11), the expression for $\tilde{\eta}_r(s)$ will lead to large numerical uncertainties for small s. This has also been noted by Evans and Hanley,[9] and they have suggested the following functional form for $\tilde{\eta}_r(s)$:

$$\tilde{\eta}_r(s)=\frac{\tilde{\eta}_r(0)}{1+s\tau}, \tag{13}$$

where τ is the relaxation time. By substituting Eq. (13) into Eq. (11), one obtains an expression for $\tilde{C}_r(s)$,

$$\tilde{C}_r(s)=\frac{\tilde{\eta}_r(0)s}{s+s^2\tau+\dfrac{4}{\rho\Theta}\tilde{\eta}_r(0)}. \tag{14}$$

Equation (14) can then be fitted to the Laplace transform of the MD simulation data, which is given by Eq. (12), by using $\tilde{\eta}_r(0)$, τ, and Θ as fitting parameters. It must be stressed that this is only valid as long as the assumption of Eq. (13) is valid and is checked in the fitting procedure.

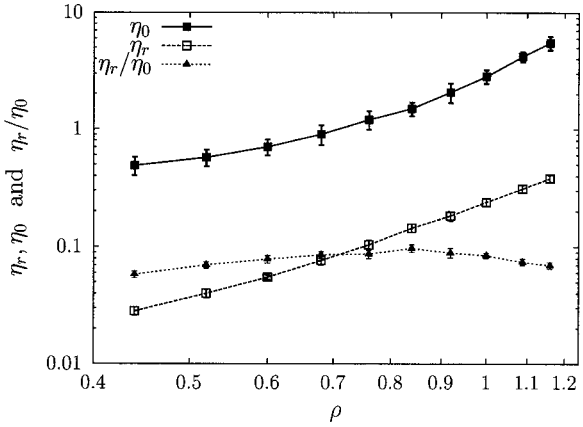

FIG. 4. Log-log plot displaying shear and rotational viscosities as a function of density for Cl_2. This log-log plot shows a good power-law relationship between η_r and ρ at $T=2.5$. Similar relationships are found for all temperatures. A power-law fit of the form $\eta_r(\rho)=a\times\rho^b$ applied to the η_r data yields $a=0.24$ $b=3.0$. The ratio η_r/η_0 peaks at approximately 10% for $\rho\approx0.84$. The shear viscosity is found to follow a stretched exponential relationship given in Eq. (20) in accordance with atomic fluids (Ref. 26). Note that for η_r, the statistical uncertainty is smaller than the plotting symbol. Lines serve as a guide for the eyes.

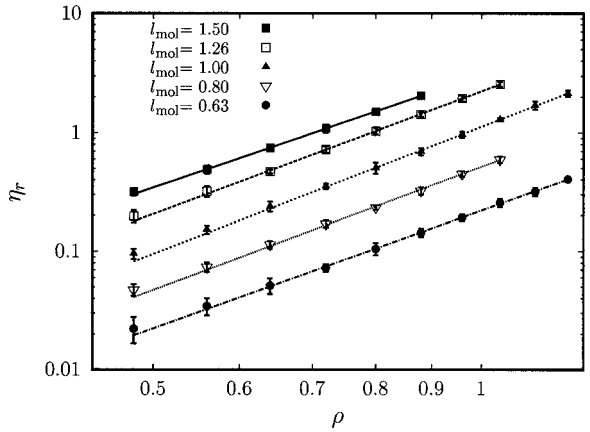

FIG. 5. Log-log plot displaying rotational viscosity as a function of density for generic molecules of various molecular lengths with $N_{UAU}=2$ and $T=2.5$. A power-law fit of the form $\eta_r(\rho)=a\times\rho^b$ has been applied to each data set. The exponent b was found to be $b=3.38\pm0.21$, where the error has been estimated as one half the difference between the maximum and minimum values. The scalar a was found to be dependent on l_{mol}.

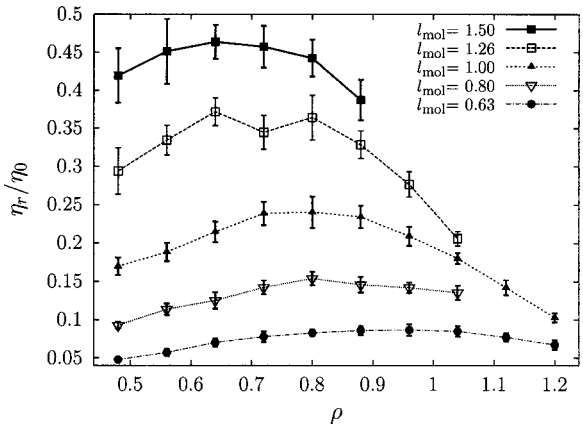

FIG. 6. Rotational viscosity for generic diatomic molecular fluids normalized against shear viscosity as a function of density for various molecular lengths at $T=2.5$. Lines serve as a guide for the eyes.

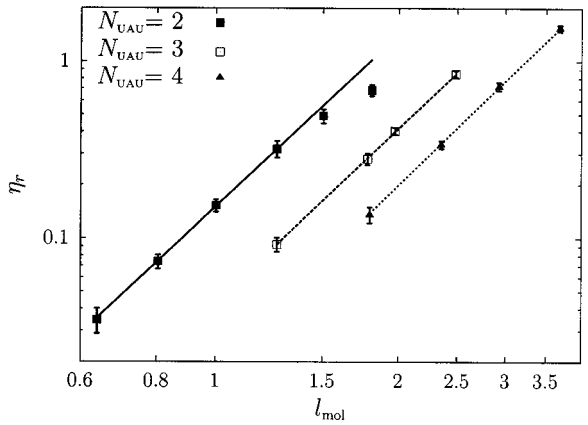

FIG. 8. Log-log plot displaying rotational viscosity as a function of molecular length at a density of 0.56 and $T=2.5$ for generic molecules with various N_{UAU}. A power-law fit of the form $\eta_r(l_{mol})=a\times l_{mol}^b$ has been applied to each data set. The exponent b was found to be $b=3.29\pm0.06$, where the error has been estimated as one half the difference between the maximum and minimum values. The scalar a was found to be dependent on N_{UAU}. The data points for $N_{UAU}=2$ at $l_{mol}=1.5, 1.8$ are beyond the reasonable limits for l_{mol} and have not been included in the fit.

III. RESULTS

A. Preliminary and corroboratory simulations

The validity of the data generated by the MD simulation program is first established by corroborating our results with previously reported values. To this end, we define the center of mass translational temperature T as[24]

$$T=\frac{\Sigma_i M_i \mathbf{v}_i^2}{(3N_{\mathrm{mol}}-3)k_B}, \tag{15}$$

where N_{mol} is the number of molecules in the system and $\mathbf{v}_i$ is the velocity of the center of mass of molecule i. Sometimes, the rotational temperature is used and for completeness, we include this[10]

$$T_r=\frac{\Sigma_i M_i \Theta_i \mathbf{\Omega}_i^2}{2N_{\mathrm{mol}}k_B}. \tag{16}$$

Recall that $\mathbf{\Omega}_i$ is the angular velocity of molecule i and is found by

$$\mathbf{\Omega}_i=\frac{\mathbf{s}_i}{\Theta_i}, \tag{17}$$

where $\mathbf{s}_i$ is the angular momentum per unit mass and Θ_i is one-third the trace of the inertial tensor $\mathbf{\Theta}_i$ per unit mass. $\mathbf{s}_i$ and $\mathbf{\Theta}_i$ are given by

$$\mathbf{s}_i=\frac{1}{M_i}\sum_{a\in i}\mathbf{r}_a\times\mathbf{p}_a, \tag{18}$$

$$\mathbf{\Theta}_i=\frac{1}{M_i}\sum_{a\in i}m_a(\mathbf{r}_a^2\mathbf{1}-\mathbf{r}_a\mathbf{r}_a), \tag{19}$$

where $\mathbf{r}_a$ is the distance between UAU a in molecule i and the center of mass and $\mathbf{p}_a$ is the momentum of UAU a. It is worth noting that since we have close to rigid uniaxial molecules, Eq. (17) is true and $\Theta_i=2I_p/3$, where I_p is the principal moment of inertia. In general, the angular velocity must be evaluated by solving the equation $\mathbf{s}_i=\mathbf{\Theta}_i\cdot\mathbf{\Omega}_i$. The fact that the molecules are (roughly) uniaxial also reduces the number of rotational degrees of freedom to 2, hence, the factor of 2 in the denominator of Eq. (16).

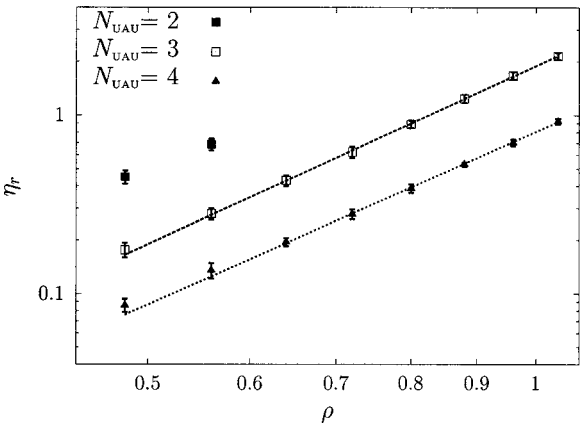

FIG. 7. Log-log plot displaying rotational viscosity as a function of density for generic molecules with $l_{mol}=1.8$ and varying N_{UAU} at $T=2.5$. A power-law fit of the form $\eta_r(\rho)=a\times\rho^b$ has been applied to each data set. The exponent b was found to be $b=3.27\pm0.05$, where the error has been estimated as one half the difference between the maximum and minimum values. The scalar a was found to be dependent on N_{UAU}. Not enough data are available to generate a fit for $N_{UAU}=2$, however, the available data are shown.

The chlorine state point given in Table I, and is hereafter referred to as S1 (note that Delhommelle[10] refers to this state point as S2), has been variously studied[10,14] and is, therefore, used for validating our method. To allow a comparison, the molecular model for chlorine used in this work is similar to that employed by Matin *et al.*[14] and Delhommelle,[10] although we allow for bond vibrations as previously mentioned. Our methods for calculating η_0 and η_r were described in Sec. II B. Figure 1 displays an autocorrelation function of the antisymmetric part of the pressure tensor for chlorine at S1 and k_s as high as 5000. A fit of Eq. (14) to the Laplace transformed MD data given in Fig. 1 is shown in Fig. 2. It is seen that the *ad hoc* functional form suggested by Evans and Hanley[9] for $\tilde{\eta}_r(s)$ [Eq. (13)] is, indeed, suitable. This was found to be the case for all fluids studied here.

TABLE IV. Summary of the l_{mol}, η_0, and η_r data collected for generic molecules with $N_{UAU}=2,3,4$ at $T=2.5$.

	$N_{UAU}=2$			$N_{UAU}=3$			$N_{UAU}=4$		
ρ	l_{mol}	η_0	η_r	l_{mol}	η_0	η_r	l_{mol}	η_0	η_r
0.48	0.64 ± 0.01	0.47 ± 0.13	0.02 ± 0.01	1.26 ± 0.01	0.43 ± 0.06	0.06 ± 0.00	1.80 ± 0.01	0.42 ± 0.06	0.09 ± 0.01
	0.81 ± 0.01	0.51 ± 0.09	0.05 ± 0.01	1.78 ± 0.01	0.56 ± 0.08	0.18 ± 0.02	2.36 ± 0.01	0.56 ± 0.12	0.22 ± 0.01
	1.00 ± 0.01	0.57 ± 0.10	0.10 ± 0.01	1.98 ± 0.01	0.65 ± 0.08	0.26 ± 0.01	2.93 ± 0.01	0.84 ± 0.12	0.45 ± 0.02
	1.26 ± 0.01	0.68 ± 0.18	0.20 ± 0.02	2.49 ± 0.01	0.96 ± 0.11	0.53 ± 0.02	3.69 ± 0.01	1.26 ± 0.22	0.97 ± 0.06
	1.51 ± 0.01	0.76 ± 0.10	0.32 ± 0.03						
	1.81 ± 0.01	0.83 ± 0.12	0.45 ± 0.04						
0.56	0.64 ± 0.01	0.61 ± 0.14	0.03 ± 0.01	1.26 ± 0.01	0.54 ± 0.09	0.09 ± 0.01	1.79 ± 0.01	0.54 ± 0.10	0.14 ± 0.01
	0.80 ± 0.01	0.65 ± 0.11	0.07 ± 0.01	1.78 ± 0.01	0.80 ± 0.13	0.28 ± 0.02	2.35 ± 0.01	0.77 ± 0.12	0.34 ± 0.02
	1.00 ± 0.01	0.81 ± 0.09	0.15 ± 0.01	1.97 ± 0.01	0.93 ± 0.17	0.40 ± 0.02	2.93 ± 0.01	1.20 ± 0.20	0.72 ± 0.04
	1.26 ± 0.01	0.96 ± 0.15	0.32 ± 0.03	2.49 ± 0.01	1.44 ± 0.16	0.85 ± 0.04	3.67 ± 0.01	2.00 ± 0.33	1.54 ± 0.06
	1.50 ± 0.01	1.09 ± 0.20	0.49 ± 0.05						
	1.81 ± 0.01	1.24 ± 0.17	0.69 ± 0.05						
0.64	0.64 ± 0.01	0.73 ± 0.13	0.05 ± 0.01	1.26 ± 0.01	0.71 ± 0.11	0.13 ± 0.02	1.79 ± 0.01	0.70 ± 0.07	0.20 ± 0.01
	0.80 ± 0.01	0.92 ± 0.15	0.11 ± 0.01	1.77 ± 0.01	1.18 ± 0.11	0.43 ± 0.03	2.34 ± 0.01	1.06 ± 0.16	0.50 ± 0.02
	1.00 ± 0.01	1.11 ± 0.15	0.24 ± 0.02	1.97 ± 0.01	1.42 ± 0.19	0.61 ± 0.03	2.92 ± 0.01	1.69 ± 0.19	1.10 ± 0.06
	1.26 ± 0.01	1.27 ± 0.13	0.47 ± 0.02	2.48 ± 0.01	2.25 ± 0.28	1.29 ± 0.06	3.68 ± 0.01	2.86 ± 0.61	2.33 ± 0.11
	1.50 ± 0.01	1.61 ± 0.16	0.74 ± 0.04						
0.72	0.63 ± 0.01	0.94 ± 0.16	0.07 ± 0.01	1.25 ± 0.01	0.89 ± 0.15	0.19 ± 0.02	1.78 ± 0.01	0.86 ± 0.07	0.28 ± 0.02
	0.80 ± 0.01	1.20 ± 0.15	0.17 ± 0.01	1.77 ± 0.01	1.60 ± 0.17	0.62 ± 0.05	2.33 ± 0.01	1.55 ± 0.13	0.73 ± 0.03
	1.00 ± 0.01	1.48 ± 0.21	0.35 ± 0.02	1.96 ± 0.01	2.03 ± 0.23	0.90 ± 0.05	2.91 ± 0.01	2.43 ± 0.36	1.59 ± 0.06
	1.26 ± 0.01	2.10 ± 0.33	0.72 ± 0.05	2.48 ± 0.01	3.40 ± 0.33	1.87 ± 0.04	3.68 ± 0.01	4.62 ± 0.46	3.43 ± 0.11
	1.51 ± 0.01	2.39 ± 0.35	1.09 ± 0.09						
0.80	0.63 ± 0.01	1.27 ± 0.22	0.10 ± 0.01	1.25 ± 0.01	1.19 ± 0.11	0.26 ± 0.01	1.77 ± 0.01	1.22 ± 0.15	0.39 ± 0.02
	0.79 ± 0.01	1.52 ± 0.16	0.23 ± 0.01	1.76 ± 0.01	2.38 ± 0.41	0.89 ± 0.04	2.32 ± 0.01	2.11 ± 0.29	1.02 ± 0.04
	0.99 ± 0.01	2.12 ± 0.55	0.51 ± 0.06	1.95 ± 0.01	3.13 ± 0.41	1.29 ± 0.05	2.90 ± 0.01	3.68 ± 0.41	2.28 ± 0.06
	1.26 ± 0.01	2.84 ± 0.37	1.03 ± 0.06	2.47 ± 0.01	5.30 ± 0.48	2.67 ± 0.07			
	1.51 ± 0.01	3.41 ± 0.50	0.50 ± 0.10						
0.88	0.62 ± 0.01	1.67 ± 0.21	0.14 ± 0.01	1.24 ± 0.01	1.66 ± 0.32	0.36 ± 0.02	1.77 ± 0.01	1.60 ± 0.22	0.53 ± 0.01
	0.79 ± 0.01	2.23 ± 0.40	0.32 ± 0.02	1.75 ± 0.01	3.51 ± 0.35	1.24 ± 0.07	2.31 ± 0.01	2.98 ± 0.50	1.38 ± 0.05
	0.99 ± 0.01	2.97 ± 0.41	0.69 ± 0.05	1.94 ± 0.01	4.63 ± 0.33	1.78 ± 0.06	2.88 ± 0.01	5.69 ± 0.74	3.12 ± 0.11
	1.25 ± 0.01	4.36 ± 0.59	1.43 ± 0.07	2.47 ± 0.01	8.83 ± 1.09	3.65 ± 0.12			
	1.51 ± 0.01	5.31 ± 0.68	2.05 ± 0.14						
0.96	0.62 ± 0.01	2.22 ± 0.42	0.19 ± 0.01	1.23 ± 0.01	2.32 ± 0.36	0.47 ± 0.04	1.76 ± 0.01	2.20 ± 0.24	0.70 ± 0.03
	0.78 ± 0.01	3.17 ± 0.30	0.45 ± 0.02	1.73 ± 0.01	5.23 ± 0.40	1.66 ± 0.08	2.29 ± 0.01	4.13 ± 0.68	1.85 ± 0.05
	0.98 ± 0.01	4.62 ± 0.57	0.96 ± 0.06	1.93 ± 0.01	7.30 ± 1.06	2.43 ± 0.08	2.86 ± 0.01	9.80 ± 1.10	4.17 ± 0.15
	1.25 ± 0.01	7.06 ± 0.85	1.95 ± 0.11						
1.04	0.61 ± 0.01	3.03 ± 0.55	0.26 ± 0.02	1.22 ± 0.01	3.00 ± 0.27	0.62 ± 0.03	1.74 ± 0.01	2.88 ± 0.36	0.92 ± 0.03
	0.77 ± 0.01	4.41 ± 0.75	0.59 ± 0.04	1.72 ± 0.01	7.85 ± 0.57	2.14 ± 0.10	2.27 ± 0.01	5.84 ± 0.98	2.39 ± 0.12
	0.97 ± 0.01	7.17 ± 0.54	1.29 ± 0.04	1.92 ± 0.01	12.9 ± 1.63	3.16 ± 0.07			
	1.25 ± 0.01	12.5 ± 1.58	2.56 ± 0.12						
1.12	0.60 ± 0.01	4.11 ± 0.53	0.32 ± 0.03						
	0.96 ± 0.01	12.0 ± 1.33	1.70 ± 0.14						
1.20	0.59 ± 0.01	6.03 ± 0.90	0.40 ± 0.02						
	0.95 ± 0.01	20.9 ± 1.71	2.15 ± 0.13						

Figure 3 shows the effect of varying k_s on η_0 and η_r for chlorine at S1, where both viscosities are normalized with respect to their maximum values. Both the shear and rotational viscosities asymptotically increase to a maximum value as the stiffness of the molecules is increased. Similar results are observed for the pressure p. The results for chlorine at S1 with $k_s=5000$ are summarized in Table II along with previously reported values for fixed bond lengths. The values for p, η_0, and η_r are all in good agreement with previously published data; i.e., for sufficiently large k_s, the viscous properties in the fluid are the same as those composed of completely rigid bonded molecules. For model

polymer melts, it has also been reported that the shear viscosity and self-diffusivity is almost independent of whether the bond is flexible or rigid;[25] i.e., the transport properties are only very slightly affected by the choice of molecular model. From Fig. 3, it can be seen that η_0 and η_r similarly behave with respect to k_s and, hence, the ratio η_r/η_0 is roughly preserved for all values of k_s. We will, therefore, use $k_s=500$ throughout the remainder of this paper.

B. Rotational viscosities for different fluids at different state points

To examine the dependence of rotational viscosity on temperature and density, η_r was evaluated at different state points. Relatively high temperatures were used for the simulations to avoid any possible phase transitions for chlorine at high densities. It is expected that both the shear and rotational viscosities vary with varying temperature, and for temperatures below $T\approx 1.5$, this is observed. However, for the region of interest, $1.5\leqslant T\leqslant 4.5$ corresponding to $1.1\leqslant T_r\leqslant 3.4$, both η_0 and η_r show very little dependence on temperature (see Table III). For example, at a density $\rho=0.76$ and temperature $T=1.5$, $\eta_0=1.15\pm 0.14$ and $\eta_r=0.11\pm 0.01$; at the same density and a temperature $T=4.0$, $\eta_0=1.30\pm 0.22$ and $\eta_r=0.11\pm 0.01$. The viscosities' density dependence is much more evident. Figure 4 shows a strong power-law dependence that exists between η_r and ρ for $0.44<\rho<1.16$. A stronger dependence is evident for η_0 over the same range of densities. In fact, we have successfully fitted the data for η_0 to a stretched exponential function,

$$\eta_0 = ke^{\rho^{\beta}/\tau}, \tag{20}$$

where k, β, and τ are fitting parameters. For chlorine at $T=1.5$, we obtain $k=0.22$, $\tau=0.38$, and $\beta=1.83$, with an error sum of squares (SSE) of 2.31×10^{-2}. The stretched exponential relationship between density and shear viscosity has previously been found by Todd[26] for simple atomic fluids. It is interesting to note that the stronger than power-law relationship between η_0 and ρ causes the ratio η_r/η_0 to peak at approximately 10% for $\rho\approx 0.84$. This result is relatively temperature independent because both η_0 and η_r were found to be independent of T for $1.5\leqslant T\leqslant 4.5$.

Figure 5 shows the relationship between η_r and ρ for generic diatomic molecules of various molecular lengths l_{mol}. As with chlorine, a very good power-law relationship exists between rotational viscosity and density. The exponent b was found to be approximately constant for all data sets with $b=3.38\pm 0.21$. This value is similar to the slope of the fit applied to chlorine in Fig. 4, which was found to be $b=3.0$, indicating that b is only slightly dependent on the molecular details. For a generic molecule with $l_{\mathrm{mol}}=0.63$, the scalar a was found to be $a=0.22$ with an SSE of 7.04×10^{-5}, which correlates well with the result for chlorine: $a=0.24$ (SSE $=1.64\times 10^{-4}$). From Fig. 5, it is also seen that the scalar a is dependent on the molecular length; i.e., the larger the value of l_{mol} is, the larger the rotational viscosity is. Thus, the affinity to fulfill Eq. (1) increases with increasing density and molecular length, which is expected.

It is known from the results for chlorine that the shear viscosity has a stretched exponential relationship with density [Eq. (20)] and, therefore, the ratio η_r/η_0 is not constant in the density interval studied here. In fact, Eq. (20) also fits the generic molecular fluid and it is, therefore, not surprising to see the same result for η_r/η_0 for the generic molecular fluid with $N_{\mathrm{UAU}}=2$ (Fig. 6). However, it can be seen that for larger molecular lengths, the fraction η_r/η_0 becomes markedly more pronounced. For a fluid composed of generic diatomic molecules with $l_{\mathrm{mol}}=1.5$, η_r/η_0 approaches 50% for $\rho\approx 0.64$. This is significantly more than the maximum value of η_r/η_0 for a generic diatomic molecule with $l_{\mathrm{mol}}=0.63$ (9%). This means that η_r increases more rapidly than η_0 as a function of l_{mol}. Figure 6 also indicates that the shear viscosity tends to dramatically increase for extreme densities, causing η_r/η_0 to decrease fast in this region.

Above, it was shown that the rotational viscosity of a fluid composed of molecules with $N_{\mathrm{UAU}}=2$ is dependent on the density of the fluid via a power-law relationship. The next step is to investigate how this relationship varies for larger generic molecules. The effects of intramolecular torsion are neglected since our molecular bending angle is approximately 2.83 ± 0.39 rad. Figure 7 shows the relationship between η_r and ρ for generic molecules with various N_{UAU} but constant molecular length ($l_{\mathrm{mol}}=1.8$). The power-law fits applied to the data yield $b=3.27\pm 0.05$, which is empirically similar to the slope of the fits found for generic molecules with $N_{\mathrm{UAU}}=2$, as would be expected. However, as can be seen from Fig. 7, increasing N_{UAU} decreases the value of η_r. This phenomenon may be explained by considering the excluded volume. For constant l_{mol}, as N_{UAU} is increased, the volume excluded by a molecule along its axis increases and becomes more rodlike than barbell shaped compared to molecules where $N_{\mathrm{UAU}}=2$. This reduces the degree of the intermolecular connectivity with neighboring molecules, thereby allowing the molecule to be more unrestrained. This, in turn, enables the molecules to deviate from Eq. (1), $\nabla\mathbf{u}=2\boldsymbol{\Omega}$, a condition that the fluid will possess on average. Or differently stated: Any small fluctuation that will perturb a fluid element away from Eq. (1) will more slowly decay if the intermolecular connectivity is small (since the surrounding fluid on average fulfills the rigid body condition). Thus, a decrease in η_r is observed.

It is apparent from Figs. 5 and 7 that η_r depends on ρ via a power-law relationship with a constant exponent $b\approx 3.32$ (derived from the averages of 3.38 ± 0.21 and 3.27 ± 0.05), for generic molecules of all lengths ($l_{\mathrm{mol}}\leqslant 1.5$) and sizes ($N_{\mathrm{UAU}}\leqslant 4$). It is only the amplitude of this relationship (visible as the vertical offset in Figs. 5 and 7) that depends on l_{mol} and N_{UAU}. To further investigate and quantify this relationship, the value of η_r at $\rho=0.56$ for each of the generic molecules considered is plotted in Fig. 8. Of most interest in this plot is the relationship between η_r and l_{mol}. It was previously found that the amplitude of the function $\eta_r(\rho)$ was dependent on l_{mol}. As can be seen in Fig. 8, this dependency itself actually takes the form of a power-law relationship. The exponent in the power-law relationship $\eta_r(l_{\mathrm{mol}})$ is $b=3.29\pm 0.06$. This is remarkably similar to the exponent for $\eta_r(\rho)$, which was found to be $b\approx 3.32$. However, increasing

the density of a fluid is similar in effect to increasing the excluded volume of the participating molecules so it should not be so surprising, perhaps, that the two relationships [$\eta_r(\rho)$ and $\eta_r(l_{\mathrm{mol}})$] are empirically so similar. We have summarized the plotted data in Appendix A.

IV. CONCLUSION

We have successfully used the functional form for $\tilde{\eta}_r(s)$ [Eq. (13)] suggested by Evans and Hanley[9] and equilibrium MD simulations to perform a systematic study of the rotational viscosity for different linear molecular fluids as a function of temperature and density. Our study encompasses chlorine and a generic uniaxial molecule where our molecular model includes intramolecular interaction, bond stretching between adjacent UAU, and bending force. Where comparisons are possible, our results agree with previously published results.

We have found that both the shear and rotational viscosities of chlorine are roughly independent of temperature in the interval of $1.5 \leqslant T \leqslant 4.5$ and that the rotational viscosity of chlorine depends on the density via a power-law relationship with scalar $a=0.24$ and exponent $b=3.0$. From these results, the rotational viscosity of chlorine may be accurately predicted for all temperatures of $1.5 \leqslant T \leqslant 4.5$ and densities in the interval of $0.44 \leqslant \rho \leqslant 1.16$. It was also found that the ratio η_r / η_0 did not exceed 10%.

By adopting a generic molecular model, where both l_{mol} and N_{UAU} can be varied, we were also able to investigate the effect of molecular structure on the rotational viscosity of simple linear molecular fluids. We have found that the rotational viscosity of fluids composed of diatomic molecules of all sizes ($l_{\mathrm{mol}} \leqslant 1.5$) follows a power-law relationship with respect to density. This result is in agreement with our result for chlorine. However, we have also found that the rotational viscosity of molecular fluids also follows a power-law relationship with respect to molecular length. Thus, the affinity of a molecular fluid to fulfill Eq. (1) increases with increasing density and molecular length, which is expected. Finally, we found that increasing N_{UAU}, for a constant l_{mol}, decreased the rotational viscosity. It is proposed that this result is due to the reduction in the intermolecular connectivity, thereby allowing the molecule to more freely deviate from Eq. (1). It is our opinion that these conclusions can be extended to fluids composed of uniaxial molecules of arbitrary length.

Additional information can be obtained by comparing the data presented here with predictions from kinetic theory. For example, the contribution from the uncorrelated collisions could be extracted this way. As mentioned in the Introduction, Allen *et al.*[11] give the kinetic theory expression for η_r in the case where the fluid is composed of convex bodies. However, before a comparison with the present data can be made, expressions for the correct molecular geometries must first be elucidated.

APPENDIX A: DENSITY AND MOLECULAR LENGTH DEPENDENCE FOR THE GENERIC FLUID

Table IV summarizes the density and molecular dependence for the generic fluid.

[1] S. R. de Groot and P. Mazur, *Non-equilibrium Thermodynamics* (Dover, New York, 1984).
[2] A. C. Eringen, *Contribution to Mechanics* (Pergamon, New York, 1969).
[3] D. J. Evans and W. B. Streett, Mol. Phys. **36**, 161 (1978).
[4] D. Tritton, *Physical Fluid Dynamics* (Oxford Science, Oxford, 1988).
[5] R. Edberg, D. J. Evans, and G. P. Morriss, Mol. Phys. **62**, 1357 (1987).
[6] J. S. Hansen, B. D. Todd, and P. J. Daivis, Phys. Rev. E (accepted for publication).
[7] S. Sarman and D. J. Evans, J. Chem. Phys. **99**, 9021 (1993).
[8] H. Kneppe, F. Schneider, and N. K. Sharma, J. Chem. Phys. **77**, 3203 (1982).
[9] D. J. Evans and H. J. M. Hanley, Phys. Rev. A **25**, 1771 (1982).
[10] J. Delhommelle, Mol. Phys. **100**, 3479 (2002).
[11] M. P. Allen, P. J. Camp, C. P. Mason, G. T. Evans, and A. J. Masters, J. Chem. Phys. **105**, 11175 (1996).
[12] A. Zakharov, A. Komolkin, and A. Maliniak, Phys. Rev. E **59**, 6802 (1999).
[13] M. I. Capar and E. Cebe, Chem. Phys. Lett. **407**, 454 (2005).
[14] M. L. Matin, P. J. Daivis, and B. D. Todd, J. Chem. Phys. **113**, 9122 (2000).
[15] J. D. Weeks, D. Chandler, and H. C. Andersen, J. Chem. Phys. **54**, 5237 (1971).
[16] J. H. R. Clarke, in *Computer Modelling of Fluids Polymers and Solids*, NATO Advance Studies Institute, Series C:293 Vol. 293 edited by C. R. A. Catlow, S. C. Parker, and M. P. Allen (Kluwer Academic, Dordrecht, 1990).
[17] D. Rapaport, *The Art of Molecular Dynamics Simulation* (Cambridge University Press, Cambridge, 1995).
[18] M. P. Allen and D. J. Tildesley, *Computer Simulation of Liquids* (Clarendon, New York, 1989).
[19] D. Frenkel and B. Smit, *Understanding Molecular Simulation* (Academic, New York, 1996).
[20] M. P. Allen, Mol. Phys. **52**, 705 (1984).
[21] B. D. Todd and P. J. Daivis, Mol. Simul. **33**, 189 (2007).
[22] J. P. Hansen and I. R. McDonald, *Theory of Simple Liquids* (Academic, New York, 1986).
[23] D. J. Evans and G. P. Morriss, *Statistical Mechanics of Nonequilibrium Liquids* (Academic, New York, 1990).
[24] R. Edberg, D. J. Evans, and G. P. Morriss, J. Chem. Phys. **84**, 6933 (1986).
[25] T. A. Hunt, Ph.D. thesis, Swinburne University of Technology, 2008.
[26] B. D. Todd, Phys. Rev. E **72**, 041204 (2005).